ANTI-TGFβ THERAPY WITH BETAGLYCAN-DERIVED P144 PEPTIDE GENE DELIVERY PREVENTS THE FORMATION OF AORTIC ANEURYSM IN A MOUSE MODEL OF MARFAN SYNDROME

Cristina Arce[1], Isaac Rodríguez-Rovira[1], Karo De Rycke[1], Karina Durán[2], Victoria Campuzano[1,3], Isabel Fabregat[4], Francesc Jiménez-Altayó[5], Pedro Berraondo[6,7], and Gustavo Egea[1,8]

[1]Department of Biomedical Sciences, School of Medicine and Health Sciences, University of Barcelona, Barcelona (Spain); [2]Department of Cardiology, Hospital Clínic y Provincial de Barcelona, Barcelona (Spain); [3]Centro de Investigación Biomédica en Red de Enfermedades Raras (CIBERER), ISCIII, Spain; [4]Bellvitge Biomedical Research Institute (IDIBELL) and Centro de Investigación Biomédica en Red de Enfermedades Hepático-Digestivas (CIBEREHD), ISCIII, Spain; [5]Department of Therapeutic Pharmacology and Toxicology, School of Medicine, Neuroscience Institute, Autonomous University of Barcelona, Bellaterra, Barcelona, (Spain); [6]Program of Immunology and Immunotherapy, CIMA University of Navarra, Pamplona (Spain); [7]Navarra Institute for Health Research (IDISNA), Pamplona (Spain); [8]August Pi i Sunyer Biomedical Research Institute (IDIBAPS-UB), Barcelona (Spain)

Running title: P144 peptide-based therapy in Marfan syndrome

Correspondence to:

Gustavo Egea, Departamento de Biomedicina, Facultad de Medicina y Ciencias de la Salud, Universidad de Barcelona, c/ Casanova 143, 08036 Barcelona (Catalunya, Spain), email: gegea@ub.edu, Phone: (+34) 934021909

Keywords: Marfan syndrome, aortic aneurysm, TGFβ, adeno-associated vector, gene therapy, P144, betaglycan

Subject terms: cell therapy, cell signaling/signal transduction, aneurysm, mechanisms,

vascular disease.

Total number of figures and tables: 6 figures (5 figures and 8 Tables in online supplementary material)

TOC category: Basic and Translational study.

TOC subcategory: Vascular Biology

ABSTRACT

Objective. We investigated the effect of a potent TGFβ inhibitor peptide (P144) from the betaglycan/TGFβ receptor III on aortic aneurysm development in a Marfan syndrome (MFS) mouse model.

Approach and Results. We used a chimeric gene encoding the P144 peptide linked to apolipoprotein A-I via a flexible linker expressed by a hepatotropic adeno-associated vector. Two experimental approaches were carried out: (i) a preventive treatment where the vector was injected before the onset of the aortic aneurysm (aged 4 weeks) and followed-up for 4 and 20 weeks, and (ii) a palliative treatment where the vector was injected once the aneurysm was formed (8 weeks-old) and followed-up for 16 weeks. We evaluated the aortic root diameter by echocardiography, the aortic wall architecture and TGFβ signaling downstream effector expression of pSMAD2 and pERK1/2 by immunohistomorphometry, and *Tgfβ1* and *Tgfβ2* mRNA expression levels by RT-PCR. MFS mice subjected to the preventive approach showed no aortic dilation in contrast to untreated MFS mice, which at the same endpoint age already presented the aneurysm. In contrast, the palliative treatment with P144 did not halt aneurysm progression. P144 improved in all cases the elastic fiber morphology and normalized the pERK1/2-mediated TGFβ signaling. Unlike the palliative treatment, the preventive one reduced the *Tgfβ1* and *Tgfβ2* mRNA levels.

Conclusions. P144 prevents the onset of aortic aneurysm but not progression once the aneurysm is formed. Results indicate the importance of reducing the excess of active TGFβ signaling during the early stages of aortic disease progression.

Abbreviations

AAV: adeno-associated virus/vector

AngII: angiotensin II

LOS: losartan

MFS: Marfan syndrome

P144: AAVApolinkerP144

PE: preventive treatment

PA: palliative treatment

PS: physiological serum

TGFβ: Transforming growth factor beta

VSMC: vascular smooth muscle cells

INTRODUCTION

Marfan syndrome (MFS) is a severe, systemic genetic disorder of the connective tissue that causes aortic aneurysm, ocular lens dislocation, emphysema and bone overgrowth[1,2,3,4,5,6,7]. MFS is caused by heterozygous mutations in the fibrillin-1 gene (*FBN1*)[8,9]. The most characteristic cardiovascular structural manifestation of MFS is found in the aortic root and the ascending aorta, where the aortic wall is dilated, and the tunica media shows fragmentation, disorganization and loss of elastic fibers[10,11,12]. *FBN1* mutations lead to progressive weakening and dilation of the aortic root and its subsequent rupture and dissection. However, it is accepted that clinical manifestations of MFS arise not only due to the abnormal structural properties of fibrillin-1 microfibrils, but also to dysregulation of TGFβ signaling, which is primarily caused by the loss of microfibrils as a reservoir for latent TGFβ[13,14,15,16]. This view was formed thanks to the availability of mouse models with reduced *FBN1* expression. In MFS patients and mice, an increase was seen in the active form of TGFβ[17,18,19,20]. Furthermore, neutralizing anti-TGFβ antibodies prevented aortic aneurysm growth in a mouse model of MFS[21,22]. In MFS, excessive TGFβ signaling enhances proteolysis of the ECM, apoptosis and phenotypic differentiation of vascular smooth muscle cells (VSMC), as well as (trans)differentiation of VSMC and fibroblasts to myofibroblasts[14,20,23]. TGFβ mediates its effects through ligand binding to a receptor that initiates signaling via phosphorylation of SMADs or ERK1/2 proteins (among others)[24,25]. However, the hyperactivation of TGFβ signaling as a determinant trigger factor of aneurysm formation has been experimentally questioned[26] based on the following observations: (i) the treatment of Marfan mice (*Fbn1*$^{mgR/mgR}$) with an anti-TGFβ antibody (1D11) was associated with a trend to disrupt, rather than prevent, aortic wall structure and aneurysm in early stages[22]; (ii) no differences were detected in active TGFβ or pSMAD levels in latent TGFβ binding protein 3 in the observed reduced aortopathy in Marfan mice in a LTBP3 knock-out background[27]; (iii) TGFβ receptor II

disruption in postnatal VSMC accelerated aneurysm growth and impaired aortic wall homeostasis[28]; and (iv) young MFS mice showed aortic dilation without altered TGFβ signaling in aortic VSMC. Moreover, aortic dilation and tunica media structural disruption were exacerbated by superimposed deletion of TGFβRII with the concomitant decreased activation of VSMC TGFβ signaling[29]. Besides disputed dysregulation of TGFβ signaling, other molecular mechanisms suggested as determinants in aortic pathogenesis include abnormal mechanosensing of aortic wall stress mediated by increased angiotensin II (AngII) signaling and VSMC phenotypic switching[20,30,31,32,33,34]. Free active and/or latent ECM-linked TGFβ superfamily ligands interact with a variety of plasma membrane receptors of the aortic mural cells (mainly VSMC). Receptors are type I (TβRI/ALKs), type II (TβRII) and type III (TβRIII/betaglycan)[35]. Betaglycan is a proteoglycan that contains a large extracellular domain, a single-pass transmembrane region and a short cytoplasmic domain, and is the most abundant TGFβ receptor in many cell types[36,37]. Betaglycan was shown to bind all three TGFβ isoforms (TGFβ1, β2 and β3) with near nanomolar affinity, but with a slight preference for TGFβ2[38], which binds TβRII with an affinity 200–500 fold weaker than TGFβ1[38,39,40]. The betaglycan ectodomain undergoes shedding, which renders both membrane-bound and soluble forms. The membrane-bound form serves as a TGFβ signaling agonist, acting as a local reservoir for TGFβ ligands, as well as presenting them to other TGFβ superfamily receptors (types I and II), which modulate the resulting signaling output. In contrast, the soluble form of betaglycan binds ligands in the extracellular space and effectively reduces this ligand's availability to cell surface signaling receptors, thus inhibiting downstream signaling[41]. For this reason, soluble betaglycan was postulated as a potential therapeutic target to control TGFβ superfamily signaling responses.

Many therapeutic strategies have been developed to interfere with TGFβ signaling and almost every component of the TGFβ pathway has been targeted for drug

development[42,43]. Among others, ligand-competitive peptides have progressed to clinical development. This is the case of the P144 peptide, which encompasses amino acids 730–743 from the TGFβ domain of the membrane and soluble forms of betaglycan[44]. The rationale for its use as a potential therapeutic drug is based on the peptide imitating soluble betaglycan, sequestering TGFβ from transmembrane signaling receptors and consequently antagonizing TGFβ stimulatory signaling[44]. Importantly, in the presence of P144, the TGFβ signaling response is not fully abolished, but simply reduced. This avoids potential undesirable secondary effects associated with the absence of TGFβ, such as the mid- to long-term risk of tumor promotion after using neutralizing anti-TGFβ antibodies or anti-TGFβ receptors I/II drugs[45]. P144 has been successfully used to block TGFβ-induced damage in murine models of scleroderma[46], periprosthetic capsular, cardiac, liver, pulmonary and epidural fibrosis[47-51], glioblastoma[52], hypertension[53,54], liver metastasis[55] and colon cancer[56].

Here, we evaluate P144 as a therapeutic tool to abrogate the pathogenesis of aortic aneurysm in a non-lethal mouse model of MFS (*Fbn1*$^{C1039G/+}$). However, P144 has a poor pharmacokinetic profile due to its short half-life in blood circulation[44]. To solve this problem, the peptide was fused with apolipoprotein A-I, and the resulting fusion protein expressed via an adeno-associated viral vector (AAV). A single administration of this vector therapy induced sustained expression of the transgene in the liver during the entire life of the mice[55]. The fusion protein circulates in plasma incorporated into HDLs, preventing the apolipoprotein A-I the intrinsic hydrophobicity of P144 stabilizing the peptide. This viral vector enables sustained *in vivo* transgene expression of the P144 peptide. Our work has additional interest because a recent study reported a significant increase in TβRIII/betaglycan protein levels in cultured fibroblasts from MFS patients with dominant-negative *FBN1* mutations, which in turn correlated with *Tgfβ1* mRNA expression[57].

MATERIAL AND METHODS

Please see the Major Resources Table in the Supplemental Materials.

Murine model

Fbn1$^{C1041G/+}$ mice (hereafter, MFS mice) were obtained from The Jackson Laboratory (Bar Harbor, ME 04609, USA) and used as a validated MFS animal model. MFS and sex- and age-matched wild type (WT) littermates were maintained on a C57BL/6J genetic background. All mice were housed in a controlled environment (12/12-hour light/dark cycle) and provided with *ad libitum* access to food and water. Animal care and colony maintenance conformed to the European Union (Directive 2010/63/EU) and Spanish guidelines (RD 53/2013) for the use of experimental animals. Ethical approval was obtained from the local animal ethics committee (CEEA and the Government of Catalonia, protocol approval number 9517-118/7).

Adeno-associated virus (AAV) production

AAV production was performed as previously indicated[55]. 293T cells were cotransfected with a transfer plasmid carrying the transgene of interest (ApolinkerP144) and the pDP8.ape packaging plasmid (PlasmidFactory, Bielefeld, Germany) to generate AAV particles of serotype 8 (AAV8). The transfection was performed using polyethylenimine “MAX”MW 25,000) (Polyscience, Warrington, PA) for 48 hours. Then, the virus was purified from cell lysates using an iodixanol gradient and buffer exchange with 50 ml centrifugal filters (Amicon® Ultra-15 Centrifugal Filter Concentrator, Merck, Ireland). Viral titers in terms of viral copies per milliliter (vg/ml) were determined by quantitative RT-PCR.

Quantitative RT-PCR

Total liver and ascending aorta mRNA from WT and MFS mice were isolated using TRI reagent (Sigma, Dorset, UK). Sample concentration and purity were determined in a

Nanodrop 1000 spectrophotometer (ThermoScientific). RNA was treated with DNase I and reverse-transcribed to cDNA with MMLV RT in the presence of RNase OUT (all reagents from Invitrogen) according to the manufacturer's instructions.

Expression of the AAV-ApolinkerP144 and *Tgfβ1* and *Tgfβ2* transcripts was determined by quantitative RT-PCR using SYBR Green Supermix (Bio-Rad Laboratories, Hercules, CA, USA) and specific primers for each gene (Supplementary Table 1). As *Gapdh* or *H3f3a* transcript levels remain unchanged across experimental conditions, the expression of these housekeeping genes was used to standardize gene expression. The amount of each transcript was expressed by the formula $2^{\Lambda\Lambda Ct(H3f3)-Ct(gene)}$ where C_t is the point at which gene fluorescence rises significantly above background fluorescence. RT-PCR reactions were performed using Bio-Rad reagents in accordance with the manufacturer's recommended protocol.

Study design and animal handling

To evaluate the therapeutic effect of the P144 peptide by gene transfer for the treatment of MFS-associated aortic aneurysm, 4- or 8-week-old male and female wild-type (WT) and MFS mice were infraorbitally injected with physiological serum (PS), AAV encoding luciferase (LUC) or ~~AAVApolinkerP144 (~~P144~~)~~ expression vectors[28]. Preventive (PE) and palliative (PA) experimental treatments were performed. A representative scheme of of both experimental protocols is shown in Supplementary Figure 1. In PE treatment, PS and P144 expression vector were single injected to 4-week-old WT and MFS mice until 8 weeks-old (4 weeks of treatment; PE1) and 24-week-old animals (20 weeks of treatment; PE2). For the PA treatment, PS, LUC or P144 expression vectors were single injected to 8-week-old mice until 24-weeks-old (16 weeks of treatment; PA). At the respective outcome time points, mice were subjected to echocardiographic analysis, liver and aorta were isolated, fixed for paraffin embedding or immersed in RNA Later (R-0901, Sigma Aldrich), frozen and stored at -80ºC. WT and MFS mice received a single injection of

physiological serum or the respective LUC or P144 expression vectors ($4x10^{12}$ vg/mice in PS). In the PA approach, a group of WT and MFS mice, injected or not with LUC and P144 vectors, also received losartan (LOS) and the combination of both P144 and LOS (P144+LOS). LOS was dissolved in drinking water (bottles kept away from the light) to a final concentration of 0.6 g/L, giving an estimated daily dose of 40–60 mg/kg/day.

Echocardiography

Two-dimensional transthoracic echocardiography was performed in all animals under 1.5% inhaled isoflurane. Each animal was scanned 12–24 hours before sacrifice. Images were obtained with a 10–13 MHz phased array linear transducer (IL12i GE Healthcare, Madrid, Spain) in a Vivid Q system (GE Healthcare, Madrid, Spain). Images were recorded and later analyzed offline using commercially available software (EchoPac v.08.1.6, GE Healthcare, Madrid, Spain). Proximal aortic segments were assessed in a parasternal long-axis view. The aortic root aorta diameter was measured from inner edge to inner edge in end-diastole at the level of the sinus of Valsalva. All echocardiographic measurements were carried out in a blinded manner by three independent investigators, at two different periods, and with no knowledge of genotype and treatment.

Histomorphometry

Ascending aorta segments were fixed in 10% formaldehyde and embedded in paraffin. Paraffin blocks were sectioned in 5 µm slices. The tunica media was delimited using bright field images corresponding to polarized light. Aortic elastic fiber ruptures were quantified by counting the number of big fiber breaks in tissue sections stained with Verhoeff-Van Gieson. Breaks larger than 20 µm were defined as evident large discontinuities in the normal circumferential continuity of each elastic lamina in the aortic media (see Figure 2C for a representative example). They were counted along the length of each elastic lamina for four different, representative images of two non-consecutive sections of the

same aorta. The mean was calculated for each sample and then for each animal. Images were captured using a Leica Leitz DMRB microscope (40x oil immersion objective) equipped with a Leica DC500 camera and were analyzed with Fiji Image J Analysis software. In addition, tunica media thickness was measured in the same paraffin sections. All measurements were carried out in a blinded manner by three blinded observers with no knowledge of genotype and treatment.

Immunolocalization

Consecutive 5 µm paraffin cross sections were stained with anti-Apolipoprotein A (1:50; Santa-Cruz; sc-30089), anti-pSMAD2 (1:100; 3108S, Cell Signaling) anti-pERK1/2 (1:50; 9101S, Cell Signaling) antibodies. For unmasking epitopes, sections were treated with 1M Tris-EDTA, 0.05% Tween, pH 9 for pSMAD2 and anti-Apolipoprotein A or with 10 mM sodium citrate, 0.05% tween, pH 6 for pERK1/2. Thereafter, sections were rinsed in PBS and incubated for 20 min with ammonium chloride (50 mM, pH 7.4) to block free aldehyde groups. Sections were permeabilized using 0.3% triton X-100 for 10 min and treated with BSA blocking buffer (1%) for 2 h prior to overnight incubation with the primary antibody in a humidified chamber at 4ºC. Subsequently, sections were rinsed with PBS, followed by 1 h incubation at room temperature with the secondary antibody goat anti-rabbit Alexa 647 (1:1000; Invitrogen, A-21246). Finally, sections were rinsed with PBS and counterstained with DAPI (1:10,000). Negative controls were processed in the same manner in the absence of the primary antibody. For quantitative analysis, 4 areas of each immunostained paraffin section were quantified. The mean was first calculated for each sample and then for each animal. All analyses were carried out using Image J software and an in-house developed Macro for automated image analysis from pictures taken with 40x objective magnification.

Statistical analysis

~~All the data shown in the present study is reported as means ± SEM. *n* refers to the number of mice in the *in vivo* experiments. GraphPad Prism 9 software was used for the statistical analysis, where $p \leq 0.05$ was considered significant. Normal distribution of all data was verified before parametric tests were used. For all datasets, data was analyzed with a parametric test using two-way Anova with Tukey post-test. Student's *t* test was used when only two groups were compared. The statistical test applied in each case is indicated in the figure legend.~~

All the data shown in the present study is reported as means ± SEM. *n* refers to the number of mice used for the GraphPad Prism 9 software was used for the statistical analysis, where $p \leq 0.05$ was already considered significant. Normal distribution and equal variance data were verified before parametric tests were used. Then, data was analyzed using two-way Anova with Tukey post-test for multiple comparison or Student's *t* test was used when only two groups were compared. For non-parametric test followed data, it was applied the Kruskal-Wallis test with Dunn's post-test for multiple comparison. The statistical test applied in each case is indicated in each figure legend.

RESULTS

AAVApolinkerP144 expression levels in MFS mouse tissues

ApolinkerP144 is a fusion protein that contains the anti-TGFβ peptide P144 fused via a flexible linker to the apolipoprotein A-I, the main component of high-density lipoproteins. This fusion protein is stably produced by AAV8. This serotype has the highest liver transduction efficiency in mice with a reduced immunogenicity profile[58]. To check the production of the fusion protein in MFS mice, we evaluated its expression by quantitative RT-PCR in liver and ascending aorta. As an internal control, we used the same vector containing LUC instead of P144. As expected, liver cells highly expressed the P144 fusion protein transcript. Moreover, the ascending aorta also significantly expressed the P144 transcript, although to a lesser extent than liver (Supplementary Figure 2A). Therefore,

the liver and the aorta ensure the constitutive expression and bloodstream presence of P144 fusion protein throughout the entire treatment period. To indirectly corroborate the presence of apolipoprotein A-I-P144 in the aortic wall, we carried out an immunofluorescence staining for apolipoprotein A since no anti-P144 antibodies are available. As expected, P144 injected mice ~~expressing the construct (ApolinkerP144)~~ showed more fluorescent signal in the adventitia and the media than not injected animals (supplementary Figure 2B).

Aortic aneurysm evolution in MFS mice

Before the injection of AAV, we evaluated by echocardiography the aortic root dilation in MFS mice of different ages to obtain a reference pattern of the temporal evolution of aortic aneurysm in our murine MFS model under our animal room conditions. MFS mice showed clear aortic root dilation at 8 weeks-old, which progressively increased in mice of 12 and 24 weeks-old. However, no significant changes were detected in the aortic root diameter in 4-week-old MFS mice compared with WT animals (Figure 1 and Supplementary Table 2). The aortic root growth diameter (indicated by the aortic root growth rate) between 4- and 8-week-old mice was twice that of MFS compared with WT mice (0.11±0.02 *vs.* 0.07±0.02 mm/week, respectively). For older mice, the growth was almost the same between WT and MFS mice and their respective age groups (8 *vs.* 12 and 12 *vs.* 24 weeks) (Supplementary Table 3). The analysis of results considering the sex showed no significant changes (supplementary Tables 2 and 3)

Aortic root growth, aortic wall histopathology and TGFβ signaling analysis when P144 is administered before the onset of aortic aneurysm: preventive treatment (PE).

Using echocardiography, we first analyzed whether P144 affected aneurysm formation. It was reported that P144 significantly reduces TGFβ signaling both *in vitro* and *in vivo*[44,55].

The P144 expression vector was injected into young WT and MFS mice just after weaning (4 weeks-old). At this age, the aortic root diameter in MFS mice was almost indistinguishable from that of WT mice (Figure 1). Four weeks after the P144 injection (8 weeks-old; PE1), aortic root dilation in MFS mice did not occur, in contrast to PS-treated MFS animals (Figure 2A and Supplementary Table 4). Next, we evaluated whether the absence of aortic dilation in 8 week-old P144-injected MFS mice was indeed a halt or simply a delay in aneurysm onset. To this end, 4 week-old MFS mice were injected with the P144 expression vector and the aortic root diameter examined at 24 weeks-old (20 weeks of preventive treatment; PE2). Results clearly showed that the aortic aneurysm did not form in the long term (Figure 2B and Supplementary Table 5). No significant differences were observed either between males and females (supplementary Tables 4 and 5 for PE1 and PE2, respectively). Not only was aortic aneurysm formation prevented by P144, but also the characteristic tunica media structural disarrays that usually accompany it, such as elastic lamina breaks (Figure 2C) and the augmentation of aortic wall thickness (Figure 2D and Supplementary Table 6).

In parallel to the histomorphometry analysis of the aortic wall, we examined the tunica media protein expression levels of TGFβ signaling downstream effectors pSMAD2 and pERK1/2 as representatives of the canonical and non-canonical TGFβ signaling pathways, respectively. To this end, using immunofluorescence, we evaluated the nuclear localization of both phosphorylated forms as indicative of TGFβ signaling activation. ~~P144 treatment significantly reduced the characteristic nuclear translocation of pSMAD2 and pERK1/2 that occurs in non-treated MFS mice (Figures 3A and B, respectively), being the normalization more dramatic for the latter than the former.~~

Unlike for pSMAD2, P144 treatment significantly reduced the characteristic nuclear translocation of pERK1/2 that occurs in non-treated MFS mice (Figures 3A and B, respectively).

Aortic root growth, aortic wall histopathology and TGFβ signaling analysis when P144 is administered once the aortic aneurysm is already formed: palliative treatment (PA).

Next, we evaluated the potential therapeutic effect of expressing P144 once the aneurysm is present. Initially, we carried out a pilot experiment with P144 and LUC expressing AAV vectors (Supplementary Figure 3). WT and MFS mice of 8 weeks of age were injected with the vehicle (physiological serum/PS), LUC (AAVLUC) or P144 (AAVApolinkerP144). We measured the aortic root diameter after 16 weeks of treatment in 24 week-old mice, when the aortic aneurysm is consolidated (Figure 1). Aortic root dilation occurred in PS- and LUC-injected MFS mice and it was indistinguishable from untreated animals. Note that P144-expressing MFS mice tended to show a reduction in aortic diameter, although statistical significance was not reached. Considering these preliminary echocardiographic results and knowing the intrinsic variability of aortic root diameter observed in adult mice, we increased the mouse sample size. In addition, we included losartan (LOS) and the combination of P144 and LOS (P144+LOS) (Figure 4). The aim of including LOS in parallel with P144 treatment was, on one hand, to have a comparative framework, as LOS is a well-established effective anti-aortic aneurysm treatment[21], and on the other hand, to investigate the potential effectiveness of a combined therapy. Unlike LOS, P114 treatment definitively did not reduce the aortic root diameter (Figure 4A and Supplementary Table 7). Note that P144 and LOS co-treatment produced the same reduction in aortic root diameter as LOS alone. Like for preventive treatments, no differences were observed between males and females following the palliative treatment. When analyzing the aortic wall architecture, MFS mice showed a thicker aortic wall than WT mice, and LOS fully normalized the size (Figure 4B and Supplementary Table 8). This was also the case for P144 and its combined treatment with LOS. As expected, MFS mice showed large elastic lamina breaks, but P144, LOS and P144+LOS treatments

significantly reduced their number (Figure 4C).

The MFS-PS mice group showed a TGFβ-associated hypersignaling visualized by the increased presence of pSMAD2 and pERK1/2 in VSMC nuclei in the tunica media (Figures 5A and B, respectively, and Supplementary Figure 4). This was not observed in MFS mice treated with P144, LOS or their combined treatment, whose results were highly like those obtained in treated WT animals (Figure 5A and B; see Supplementary Figure 4 for representative images). Note that P144 protein expression in WT mice was innocuous. ~~No differences were observed when results were analyzed by sex (data not shown).~~

Aortic TGFβ1 and TGFβ2 mRNA expression levels in P144-treated MFS mice

Since it was reported that betaglycan has a higher affinity for TGFβ2 than for TGFβ1 *in vitro*[40], we next evaluated whether the inhibition of aortic aneurysm formation following PE and PA treatments may have an impact on TGFβ ligands bioavailability due to changes in their gene expression. To this end, we evaluated *Tgfβ1* and *Tgfβ2* mRNA expression levels by RT-PCR in the aortic wall of treated and untreated WT and MFS mice. MFS animals showed significantly higher mRNA expression levels for both transcripts than WT mice~~, *Tgfβ1* always being more accentuated,~~ regardless of the outcome age (8 and 24 weeks-old). PE1 and PE2 treatments caused a significant reduction in the gene expression of both TGFβ ligands in MFS mice but not affecting WT ones (Figure 6A and B). ~~although the inhibitory effect was more severe for *Tgfβ2* than for *Tgfβ1*~~. Unlike the preventive treatments, the transcriptional levels of both TGFβ ligands following PA treatment were almost unaltered in MFS mice (Supplementary Figure 5). Therefore, P144 inhibits the overexpression of *Tgfβ*1 and *Tgfβ*2 in the aortic wall of MFS mice only when it is administered early in the aortic aneurysm, but not later.

DISCUSSION

We here have examined the use of betaglycan/TGFβ receptor III-derived peptide P144

as a potential new therapeutic tool to interfere in the characteristic aortic aneurysm development in MFS. To this end we have administered P144 via an AAV-based expression vector in MFS mice (C1041G/+) following a preventive (PE) or palliative (PA) approach, expressing P144 before or after the aneurysm was generated. The main results of our study are: (1) P144 is constitutively expressed both in liver (as expected) and to a lesser but significant manner in aorta as well; (2) P144 fully blocks the formation of the aneurysm, but not its progression once formed; (3) neither aortic wall disarrays nor non-canonical TGFβ hypersignaling (ERK1/2-mediated) occurred when the aneurysm was prevented by P144, and (4) P144 injected early can normalize the intrinsic abnormally high *Tgfβ1* and *Tgfβ2* mRNA expression levels in MFS mice.

Almost two decades ago, it was reported that TGFβ signaling was dysregulated in the aortic pathogenesis of MFS. This was based on the full normalization of the aortic wall in MFS mice, evaluated by echocardiography and histology using neutralizing anti-TGFβ antibodies and LOS (as AT1R activates TGFβ downstream effectors), and on the high structural similarity of fibrilin1 with LTBPs[21,59]. These observations immediately led to several clinical trials with LOS where the results were rather frustrating, as no clear improvement in aortic root progression was observed[60,61]. A short time later, new studies questioned TGFβ as a determinant primary trigger factor[62]. When our study was initiated, the TGFβ-based hypothesis was prevalent, and we postulated that the betaglycan-derived peptide P144 might be a promising therapeutic tool to regulate the abnormally increased bioavailability of active TGFβ in aortic mural cells. The use of the P144 peptide as an anti-TGFβ tool *a priori* afforded the advantage that it only causes partial inhibition of TGFβ signaling, and therefore a better safety profile than tools that completely abolish the signaling, thus in turn avoiding, to some extent, the risk of tumor formation[62]. In this respect, we observed that P144, preventively added, indeed abolished the overexpression of *Tgfβ1* and *Tgfβ2* transcripts in MFS mice without significantly affecting their normal levels in WT animals. These results indicate that only in MFS, where TGFβ

ligands are overexpressed, P144 treatment not only seems to act as a sponge of their excess, but also alters both ligands transcription, suggesting a feedback or direct regulatory effect within the wall itself. Nevertheless, this transcriptional effect is not surprising because using TGFβ inhibitors like galunisertib in liver cancer patients, it is observed that the inhibition of the TGFβ pathway by the drug is invariably accompanied by a significant reduction of the expression of TGFβ. Importantly, this behavior is used as a clinical diagnostic biomarker indicative that the treatment is working in patients (PMID: 32210440; **CRIS-**INCLUIRLA EN LAS REFERENCIAS). Moreover, changes in mRNA expression levels are not necessarily indicative of a reduced capability of P144 to sequester excessive soluble TGFβ ligands with the subsequent reduction of circulating and local aortic levels of TGFβ as it would be the case at protein level. ~~In this way P144 mimics the role of the endogenous soluble domain of betaglycan, and consequently triggers a local compensatory negative signaling response in the aorta of MFS mice. In addition, P144 administration via an AAV-based expression vector makes it especially attractive as AAVs are considered one of the most effective delivery tools for gene therapy due to their low toxicity and mild stimulation of immune responses, and they also facilitate a safe, long-term expression of the peptide[63].~~

The observation that the P144 peptide prevents aneurysm formation both in the short- and long-term, but not its progression once formed, confirms a divergent role for TGFβ in aortic aneurysm development and growth in MFS, as previously reported[22,59], but with apparent disputed effects. Ramirez's laboratory showed that the impact of TGFβ on the formation and progression of aortic aneurysm varied (protective or detrimental) depending on when cytokine activity was intercepted and on the therapeutic agent used (neutralizing anti-TGFβ antibodies or LOS). They concluded that TGFβ hypersignaling is a secondary driver of aneurysm progression in MFS, since blocking TGFβ in young MFS animals (mgR/mgR) at an early stage of the disease (2 weeks-old/P16) exacerbated the aneurysm, whereas treatment at later stages was beneficial[22]. Along the same line of

evidence, but utilizing another MFS mouse model (C1041G/+), Dichek *et al*., reported that the loss of physiologic SMC-associated TGFβ signaling enhanced aortopathy after postnatal SMC-specific deletion of TβRII[64]. Strikingly, the aortopathy developed in the absence of detectable alterations in TGFβ signaling in young MFS mice. Moreover, thoracic and abdominal aortic disease, induced after AngII infusion, were also both exacerbated when a pan-TGFβ neutralizing antibody was given to 8 to 12 week-old mice[65]. These results suggest that it is critical to maintain a physiologic basal TGFβ signaling level for early normal aortic development and that its pathologic imbalance will probably lead to the appearance of aortopathy. Our results are in accordance with this postulate, as P144 expression maintains TGFβ ligands and canonical (SMAD2) and non-canonical (ERK1/2) downstream signaling pathways at normal levels in MFS mice (C1039G/+). However, this was not the case when P144 was administered once aortic aneurysm progression had already started. It is possible, that at this stage, aortic P144 expression levels are not sufficient to reduce the overexpression and availability of bioactive soluble TGFβ ligand levels, therefore becoming detrimental. Alternatively, but not mutually exclusive, it could be that other mechanisms are involved, mainly acting at advanced stages of aneurysm progression, and which also interfere in the expression and function of TGFβ, compensating, to some extent, the local inhibitory effect of P144. This would be case of AngII-AT1R, whose TGFβ-independent dysregulated mechanisms, which participate in vascular mechanical stress, hemodynamic force and/or kinetic energy, also primarily contribute to aortic aneurysm progression[66,67,68,69]. At the same time, they could also indirectly interfere in TGFβ-associated signaling for example, SMADs pathway and/or in their own TGFβ ligand or receptor expression levels[60,70,71,72], being altogether determinant in aneurysm growth and rupture. In any case, it is clear from this and previous studies that TGFβ is relevant in aortic formation and growth, and its signaling levels are also contextually critical in the time window in which its potential therapeutic effect finally becomes detrimental or beneficial.

Our results with betaglycan-derived P144 peptide highlight recent studies in which cultured fibroblasts from MFS patients with dominant-negative *FBN1* mutations showed increased betaglycan/TβRIII protein levels, which in turn correlated with increased *Tgfβ1* mRNA expression[57]. Membrane-bound betaglycan serves as a TGFβ signaling agonist acting as a local reservoir for TGFβ ligands and promoting their subsequent high-affinity interaction with other TGFβ receptors (TβRI and TβRII), also regulating their expression and membrane internalization[73]. In contrast, soluble betaglycan predominantly acts as a ligand-binding decoy preventing the interaction of TGFβ ligands with cell surface receptors[46]. Therefore, presence in the bloodstream and local aorta expression of P144 acts as an antagonist to the intrinsic MFS-associated TGFβ hyperactivity, normalizing bioactive TGFβ ligands to physiological levels.

We are aware that our study has some limitations: (i) unlike preventive P144 treatment, the palliative approach did not reduce the aortic root diameter, conversely to the aortic wall organization and TGFβ signaling, which showed an almost total normalization. A possible explanation for this disparity is that the histological improvement might not be sufficient to have a functional (for example, mechanical) impact that can be resolved by echocardiography. However, this would not be the case for the preventive treatment in which the P144-treated mice were younger (4 weeks-old), where the aorta is not yet fully structurally and functionally developed as in 8 week-old mice, age at which the palliative treatment was started. This functional and structural disparity of results has been previously observed in MFS experimental and clinical practice[74,75] even though other studies showed a good correlation between both parameters[76,77]; (ii) we cannot discard that P144 might affect blood pressure, but it is highly unlikely because previous studies in rodents clearly stated that blood pressure was unaffected by P144 treatments[48]; (iii) most preclinical studies use the C1041G/+ mouse model, which slowly develops aortic aneurysm but rarely ends with aortic dissection. The mgR mouse model, which is a more severe model developing the disease and suitable to monitor the survival rate, would have

been more appropriate for evaluating the natural progression of aneurysm to dissection that occurs in many MFS patients; (iv) *a priori*, the preventive treatment with P144 in human patients does not seem as feasible as any other potential palliative treatment, but it cannot be discarded since it might be of help to those patients who suffer the disease but have not as yet developed the aneurysm; and (v) AAV8 is not the most suitable AAV serotype to use for vasculature, although other serotypes do not largely transduce smooth muscle cells either[78,79]. However, an AAV-based expression strategy guarantees the continuous presence of P144 in the bloodstream (mostly coming from liver cells but also locally from aortic cells), whose stability is facilitated by its linking to apolipoprotein A-I. AAV-mediated expression approach has been very recently reported for oligonucleotide to AP-1 transcription factor in MFS[80]. This work shows a significant reduction of elastolysis in MFS mice (mgR/mgR)[80] which not only highlights the relevance of AP-1 in aortic wall organization but also reinforces the potential therapeutic use of AAV-based therapy for aortic diseases. AAV vector expression technology for treating some monogenetic diseases has been applied successfully and two AAV-based drugs have received FDA approval[28], whose potential translational application is closer in time to that based on highly potential patient-derived induced pluripotent stem cells (iPSCs)-based technology[81,82,83,84]. P144 administration via an AAV-based expression vector makes it especially attractive as AAVs are considered one of the most effective delivery tools for gene therapy due to their low toxicity and mild stimulation of immune responses, and they also facilitate a safe, long-term expression of the peptide[63].

In conclusion, P144 peptide, mimicking the role of the endogenous soluble domain of betaglycan, triggers a local compensatory negative signaling response in the aorta of MFS mice and blocks the onset of aortic aneurysm, but not progression once it is already formed. This preventive effect is ~~mechanistically~~ associated with the inhibition of TGFβs1 and 2 overexpression and subsequent hypersignaling (the ERK1/2-mediated one mainly)

occurring in MFS aorta, bringing their expression levels to physiological levels. This observation is demonstrative of the importance of reducing the excess of TGFβ during early stages of aortic disease progression in MFS.

ACKNOWLEDGEMENTS

Acknowledgements: We thank Helena Kruyer for language editing.

Sources of funding: This work was supported by grants from the National Marfan Association of the United States (NMF2015), MINECO from the Spanish Government (SAF2017-83039-R) and Fondo de Investigación Sanitaria-Fondo Europeo de Desarrollo Regional (FEDER) under Grant PI19/01128. G.E. greatly acknowledges the invaluable support of Damelys Fumero and the Asociación Eutsi Gogor Danok Batera from the Basque Country for the research carried out in his lab. I.R.-R. is a Spanish predoctoral fellow (FPI program).

Disclosures: None.

HIGHLIGHTS

- P144 is a peptide derived from the extracellular domain of betaglycan/TGFβ receptor III.
- P144 is constitutively expressed in a murine model of Marfan syndrome (C1041G/+) by adeno-associated vector (AAV)-mediated gene therapy.
- P144 blocks the formation of the ascending aortic aneurysm, but not its progression once is already formed.
- P144 also prevents the aortic wall disarrays and the ERK1/2-mediated TGFβ hypersignaling occurred in MFS.
- P144 reduces the MFS-associated mRNA overexpression of TGFβs1 and 2 in the aortic wall.

SUPPLEMENTAL MATERIALS

Online Figures 1-5.

Online Supplementary Tables 1-8.

REFERENCES

1. Pyeritz, R. E. The Marfan Syndrome. Annu Rev Med. 2000; 51:481-510.

2. De Paepe, A., Devereux, R. B., Dietz, H. C., Hennekam, R. C. M., & Pyeritz, R. E. Revised diagnostic criteria for the Marfan syndrome. Am J of Med Genet. 1996; 62:417–426.

3. Loeys, B. L., Dietz, H. C., Braverman, A. C., Callewaert, B. L., De Backer, J., Devereux, R. B., Hilhorst-Hofstee, Y., Jondeau, G., Faivre, L., Milewicz, D. M., Pyeritz, R. E., Sponseller, P. D., Wordsworth, P., & De Paepe, A. M. The revised Ghent nosology for the Marfan syndrome. J Med Genet. 2010; 47:476–485.

4. Cañadas, V., Vilacosta, I., Bruna, I., & Fuster, V. Marfan syndrome. Part 1: Pathophysiology and diagnosis. Nat Rev Cardiol. 2010; 7:256–265.

5. Cañadas, V., Vilacosta, I., Bruna, I., & Fuster, V. Marfan syndrome. Part 2: Treatment and management of patients. Nat Rev Cardiol. 2010; 7:266–276.

6. De Backer, J. Marfan Syndrome and Related Heritable Thoracic Aortic Aneurysms and Dissections. Curr Pharm Des. 2015; 21:4061–4075.

7. Kodolitsch, Y. Von, De Backer, J., Schüler, H., Bannas, P., Behzadi, C., Bernhardt, A. M., Hillebrand, M., Fuisting, B., Sheikhzadeh, S., Rybczynski, M., et al. Perspectives on the revised Ghent criteria for the diagnosis of Marfan syndrome. Clin Genet. 2015; 8:137–155.

8. Dietz, H. C., Cutting, C. R., Pyeritz, R. E., Maslen, C. L., Sakai, L. Y., Corson, G. M., Puffenberger, E. G., Hamosh, A., Nanthakumar, E. J., Curristin et al. Marfan syndrome caused by a recurrent de novo missense mutation in the fibrillin gene. Nature. 1991; 352:337–339.

9. Sakai, L. Y., Keene, D. R., Renard, M., & De Backer, J. FBN1: The Disease-Causing Gene for Marfan Syndrome and Other Genetic Disorders. Gene. 2017; 591:279–291.

10. Schlatmann, T. J. M., & Becker, A. E. Pathogenesis of dissecting aneurysm of aorta. Comparative histopathologic study of significance of medial changes. Am J Cardiol. 1977; 39:21–26.

11. Hollister, D. W., & Maurice Godfrey, M. Immunohistologic abnormalities of the microfibrillar-fiber system in the Marfan Syndrome. New Eng J Med. 1990; 323(3):152-9.

12. Cook, J. R., Carta, L., Galatioto, J., & Ramirez, F. Cardiovascular manifestations in Marfan syndrome and related diseases; multiple genes causing similar phenotypes. Clin Genet. 2014; 87:11–20.

13. Dietz, H. C. TGFβ in the pathogenesis and prevention of disease: a matter of aneurysmic proportions. J Clin Invest. 2010; 120:403–407.

14. Doyle, J. J., Gerber, E. E., & Dietz, H. C. Matrix-Dependent Perturbation of TGFβ signaling and disease. FEBS Lett. 2012; 586:2003–2015.

15. Gillis, E., Van Laer, L., & Loeys, B. L. Genetics of thoracic aortic aneurysm: At the crossroad of transforming growth factor-β signaling and vascular smooth muscle cell contractility. Circ Res. 2013; 113:327–340.

16. Takeda, N., Hara, H., Fujiwara, T., Kanaya, T., Maemura, S., & Komuro, I. TGF-β signaling-related genes and thoracic aortic aneurysms and dissections. Int J Mol Sci. 2018; 192125.

17. Neptune, E. R., Frischmeyer, P. A., Arking, D. E., Myers, L., Bunton, T. E., Gayraud, B., Ramirez, F., Sakai, L. Y., & Dietz, H. C. Dysregulation of TGF-β

activation contributes to pathogenesis in Marfan syndrome. Nat Genet. 2003; 33:407–411.

18. Ng, C. M., Cheng, A., Myers, L. A., Martinez-Murillo, F., Jie, C., Bedja, D., Gabrielson, K. L., Hausladen, J. M. W., Mecham, R. P., Judge, D. P. et al. TGF-β-dependent pathogenesis of mitral valve prolapse in a mouse model of Marfan syndrome. J Clin Invest. 2004; 114:1586–1592.

19. Nataatmadja, M., West, J., & West, M. Overexpression of transforming growth factor-β is associated with increased hyaluronan content and impairment of repair in Marfan syndrome aortic aneurysm. Circulation. 2006; 114:371–377.

20. Crosas-Molist, E., Meirelles, T., López-Luque, J., Serra-Peinado, C., Selva, J., Caja, L., Gorbenko Del Blanco, D., Uriarte, J. J., Bertran, E., Mendizábal, Y. et al. Vascular smooth muscle cell phenotypic changes in patients with Marfan syndrome. Arterioscler Thromb Vas Biol. 2015; 35:960–972.

21. Habashi, J. P., Judge, D. P., Holm, T. M., Cohn, R. D., Loeys, B. L., Cooper, T. K., Myers, L., Klein, E. C., Liu, G., Calvi, C. et al. Losartan, an AT1 antagonist, prevents aortic aneurysm in a mouse model of Marfan syndrome. Science, 2006; 312:117–121.

22. Cook, J. R., Clayton, N. P., Carta, L., Galatioto, J., Chiu, E., Smaldone, S., Nelson, C. A., Cheng, S. H., Wentworth, B. M., & Ramirez, F. Dimorphic Effects of Transforming Growth Factor-β Signaling during Aortic Aneurysm Progression in Mice Suggest a Combinatorial Therapy for Marfan Syndrome. Arterioscler Thromb Vas Biol. 2015; 35(4):911–917.

23. Jones, J. A., Spinale, F. G., & Ikonomidis, J. S. Aneurysm Developmen: a Paradox in Pathogenesis. J Vasc Res. 2009; 46:119–137.

24. Shi, Y., & Massagué, J. Mechanisms of TGF-β signaling from cell membrane to the nucleus. Cell. 2003; 113:685–700.

25. Pardali, E. and Dijke, P. TGF-β Signaling and Cardiovascular Diseases. Int J Biol Sci. 2012; 8:195–213.

26. Mallat, Z., Ait-Oufella, H., & Tedgui, A. The Pathogenic Transforming Growth Factor-β Overdrive Hypothesis in Aortic Aneurysms and Dissections: A Mirage? Circ Res. 2017; 120:1718–1720.

27. Zilberberg, L., Phoon, C. K. L., Robertson, I., Dabovic, B., Ramirez, F., & Rifkin, D. B. Genetic analysis of the contribution of LTBP-3 to thoracic aneurysm in Marfan syndrome. PNAS USA. 2015; 112:14012–14017.

28. Li, C., & Samulski, R. J. Engineering adeno-associated virus vectors for gene therapy. Nat Rev Genet. 2020; 21:255–272.

29. Wei, H., Hong-Hu, J., Angelov, S., Fox, K., Yan, J., Enstrom, R., Smith, A., Dichek, D. Aortopathy in a Mouse Model of Marfan Syndrome Is not mediated by Altered Transforming Growth Factor ß signaling. JAHA. 2017; 6:e004968.

30. Humphrey, J., Milewicz, D., Tellides, G., Schwartz, M. Cell biology. Dysfunctional mechanosensing in aneurysms. Science. 2014; 344(6183):477-9.

31. Jeremy, R., Robertson, E., Lu, Y., Hambly, B. Perturbations of mechanotransduction and aneurysm formation in heritable aortopathies. Int J Cardiol. 2013; 169:7-16.

32. Nolasco, P., Golçalves-Fernandes, C., Ribeiro-Silva, J.C., Oliveira, P., Sacrini, M, Vasconcelos de Brito, I., Coralie de Bessa, T., Pereira, L., Tanaka, L., Alencar, A. et al. Impaired vascular smooth muscle cell force-generating capacity and phenotypic deregulation in Marfan Syndrome mice. Biochim Biophys Acta Mol Basis Dis. 2020; 1866:165587.

33. Dale, M., Fitzgerald, M., Liu, Z., Meisinger, T., Karpisek, A., Purcell, L., Carson, J., Harding, P., Lang, H., Koutakis, P. et al. Premature aortic smooth muscle cell differentiation contributes to matrix dysregulation in Marfan Syndrome. PLoS One. 2017; 12:e0186603.

34. Michel, J. B., Jondeau, G., Milewicz, D. From genetics to response to injury: vascular smooth muscle cells in aneurysms and dissections of the ascending aorta. Cardiovasc Res. 2018; 114:578-589.

35. Nickel, J., Ten Dijke, P., & Mueller, T. D. TGF-β family co-receptor function and signaling. Acta Bioch Bioph Sin. 2018; 50:12–36.

36. López-Casillas, F., Cheifetz, S., Doody, J., Andres, J. L., Lane, W. S., & Massagué, J. Structure and expression of the membrane proteoglycan betaglycan, a component of the TGF-β receptor system. Cell. 1991; 67:785–795.

37. Wang, X. F., Lin, H. Y., Ng-Eaton, E., Downward, J., Lodish, H. F., & Weinberg, R. A. Expression cloning and characterization of the TGF-β type III receptor. Cell. 1991; 67:797–805.

38. Kyung Kim, S., Henen, M., Hinck, A. Structural biology of betaglycan and endoglin, membrane-bound co-receptors of the TFG-beta family. Exp Biol Med (Maywood). 2019; 244:1547-1558.

39. Bilandzic, M., & Stenvers, K. L. Betaglycan: A multifunctional accessory. Mol Cell Endocrinol. 2011; 339:180–189.

40. Mendoza, V., Vilchis-Landeros, M., Mendoza-Hernandez, G., Huang, T., Villarreal, M., Hinck, A., López-Casillas, F., Montiel, J-L. Betaglycan has two independent domains required for high affinity TGF-ß binding: proteolytic cleavage separates the domains and inactivates the neutralizing activity of the soluble receptor. Biochemistry. 2009; 48:11755–11765.

41. López-Casillas, F., Payne, H. M., Andres, J. L., & Massagué, J. Betaglycan can act as a dual modulator of TGF-β access to signaling receptors: Mapping of ligand binding and GAG attachment sites. J Cell Biol. 1994; 124:557–568.

42. Akhurst, R. J., & Hata, A. Targeting the TGFβ signalling pathway in disease. Nat Rev Drug Discov. 2012; 11:790–811.

43. Wagner, A. H., Zaradzki, M., Arif, R., Remes, A., Müller, O. J., & Kallenbach, K. Marfan syndrome: A therapeutic challenge for long-term care. Biochem Pharmacol. 2019; 164:53–63.

44. Dotor, J., López-Vázquez, A. B., Lasarte, J. J., Sarobe, P., García-Granero, M., Riezu-Boj, J. I., Martínez, A., Feijoó, E., López-Sagaseta, J., Hermida, J. et al. Identification of peptide inhibitors of transforming growth factor beta 1 using a phage-displayed peptide library. Cytokine. 2007; 39:106–115.

45. Llopiz, D., Dotor, J., Casares, N., Bezunartea, J., Díaz-Valdés, N., Ruiz, M., Aranda, F., Berraondo, P., Prieto, J., Lasarte, J. J. et al. Peptide inhibitors of transforming growth factor-β enhance the efficacy of antitumor immunotherapy. Int J Cancer. 2009; 125:2614–2623.

46. Santiago, B., Gutierrez-Cañas, I., Dotor, J., Palao, G., Lasarte, J. J., Ruiz, J., Prieto, J., Borrás-Cuesta, F., & Pablos, J. L. Topical application of a peptide inhibitor of transforming growth factor-β1 ameliorates bleomycin-induced skin fibrosis. J Invest Dermatol. 2005; 125:450–455.

47. Ruiz-De-Erenchun, R., Dotor De Las Herrerías, J., & Hontanilla, B. Use of the transforming growth factor-β1 inhibitor peptide in periprosthetic capsular fibrosis: Experimental model with tetraglycerol dipalmitate. Plast Reconstr Surg. 2005; 116:1370–1378.

48. Hermida, N., López, B., González, A., Dotor, J., Lasarte, J. J., Sarobe, P., Borrás-Cuesta, F., & Díez, J. A synthetic peptide from transforming growth factor-β1 type III receptor prevents myocardial fibrosis in spontaneously hypertensive rats. Cardiovasc Res. 2009; 81:601–609.

49. Ezquerro, I. J., Lasarte, J. J., Dotor, J., Castilla-Cortázar, I., Bustos, M., Peñuelas, I., Blanco, G., Rodríguez, C., Lechuga, M. D. C. G., Greenwel, P., et al. A synthetic peptide from transforming growth factor β type III receptor inhibits liver fibrogenesis in rats with carbon tetrachloride liver injury. Cytokine. 2003; 22:12–20.

50. Arribillaga, L., Dotor, J., Basagoiti, M., Riezu-Boj, J. I., Borrás-Cuesta, F., Lasarte, J. J., Sarobe, P., Cornet, M. E., & Feijoó, E. Therapeutic effect of a peptide inhibitor of TGF-β on pulmonary fibrosis. Cytokine. 2011; 53:327–333.

51. Albiñana-Cunningham, J. N., Ripalda-Cemboráin, P., Labiano, T., Echeveste, J. I., Granero-Moltó, F., & Alfonso-Olmos, M. Mechanical barriers and transforming growth factor beta inhibitor on epidural fibrosis in a rabbit laminectomy model. J Orthop Surg Res. 2018; 13:1–7.

52. Gallo-Oller, G., Vollmann-Zwerenz, A., Meléndez, B., Rey, J. A., Hau, P., Dotor, J., & Castresana, J. S. P144, a Transforming Growth Factor beta inhibitor peptide, generates antitumoral effects and modifies SMAD7 and SKI levels in human glioblastoma cell lines. Cancer Lett. 2016; 381:67–75.

53. Baltanás, A., Miguel-Carrasco, J. L., San José, G., Cebrián, C., Moreno, MU., Dotor, J., Borrás-Cuesta, F., López, B., González, A., Díez, J., Fortuño, A. et al. A synthetic peptide from transforming growth factor-β1 Type III receptor inhibits NADPH oxidase and prevents oxidative stress in the kidney of spontaneously hypertensive rats. Antioxid Redox Sign. 2013; 19:1607–1618.

54. Miguel-Carrasco, J. L., Baltanás, A., Cebrián, C., Moreno, M. U., López, B., Hermida, N., González, A., Dotor, J., Borrás-Cuesta, F., Díez, J. et al. Blockade of TGF-β 1 signalling inhibits cardiac NADPH oxidase overactivity in hypertensive rats. Oxid Med Cell Longev. 2012; 2012:726940.

55. Medina-Echeverz, J., Fioravanti, J., Diáz-Valdés, N., Frank, K., Aranda, F., Gomar, C., Ardaiz, N., Dotor, J., Umansky, V., Prieto, J. et al. Harnessing high density lipoproteins to block transforming growth factor beta and to inhibit the growth of liver tumor metastases. PLoS ONE. 2014; 9:1–9.

56. Medina-Echeverz, J., Vasquez, M., Gomar, C., Ardaiz, N., & Berraondo, P. Overexpression of apolipoprotein A-I fused to an anti-transforming growth factor beta peptide modulates the tumorigenicity and immunogenicity of mouse colon cancer cells. Cancer Immunol Immunother. 2015; 64:717–725.

57. Groeneveld, M. E., Bogunovic, N., Musters, R. J. P., Tangelder, G. J., Pals, G., Wisselink, W., Micha, D., & Yeung, K. K. Betaglycan (TGFBR3) up-regulation correlates with increased TGF-β signaling in Marfan patient fibroblasts in vitro. Cardiovasc Pathol. 2018; 32:44–49.

58. Nakai, H., Fuess, S., Storm, T. A., Muramatsu, S -i., Nara, Y., & Kay, M. A. Unrestricted Hepatocyte Transduction with Adeno-Associated Virus Serotype 8 Vectors in Mice. J Virol. 2005; 79:214–224.

59. Milewicz, Di. M., & Ramirez, F. Therapies for Thoracic Aortic Aneurysms and Acute Aortic Dissections: Old Controversies and New Opportunities. Arterioscler Thromb Vas Biol. 2019; 39:126–136.

60. Milewicz, Di. M., Prakash S. K., & Ramirez, F. Therapeutics Targeting Drivers of Thoracic Aortic Aneurysms and Acute Aortic Dissections: Insights from Predisposing Genes and Mouse Models. Annu Rev Med. 2017; 68:51–67.

61. Hoffman Bowman, M., Eage, K. A., Milewicz, D. M. Update on Clinical Trials of Losartan with and without ß-blockers to block aneurysm growth in patients with Marfan Syndrome: A Review. JAMA Cardiol. 2019; 4:702-707.

62. Tellides, G. Further evidence supporting a protective role of transforming growth factor-β (TGFβ) in aortic aneurysm and dissection. Arterioscler Thromb Vasc Biol. 2017; 37: 1983–1986.

63. Samulski, R. J., Muzyczka, N. AAV-Mediated Gene Therapy for Research and Therapeutic Purposes. Annu Rev Virol. 2014; 427-51.

64. Hu, J. H., Wei, H., Jaffe, M., Airhart, N., Du, L., Angelov, S. N., Yan, J., Allen, J. K., Kang, I., Wight, T. N. et al. Postnatal deletion of the type II transforming growth factor-β receptor in smooth muscle cells causes severe aortopathy in mice. Arterioscler Thromb Vasc Biol. 2015; 35:2647–2656.

65. Wang, Y., Ait-Oufella, H., Herbin, O., Bonnin, P., Ramkhelawon, B., Taleb, S., Huang, J., Offenstadt, G., Combadière, C., Rénia, L. et al. TGF-beta activity protects against inflammatory aortic aneurysm progression and complications in angiotensin II-infused mice. J Clin Invest. 2010; 120:422–432.

66. Humphrey, J. D., Schwartz, M. A., Tellides, G., Milewicz, D. M. Role of mechanotransduction in vascular biology: focus on thoracic aortic aneurysms and dissections. Circ Res. 2015; 116:1448–1461.

67. Milewicz, D. M., Trybus, K. M., Guo, D. C., Sweeney, H. L., Regalado, E., Kamm, K., Stull, J. T. Altered smooth muscle cell force generation as a driver of thoracic aortic aneurysms and dissections. Arterioscler Thromb Vasc Biol. 2017; 37:26–34.

68. Ramirez, F., Caescu, C., Wondimu, E., Galatioto, J. Marfan syndrome; A connective tissue disease at the crossroads of mechanotransduction, TGFβ signaling and cell stemness. Matrix Biol. 2018; 71-72:82–89.

69. Dorst, D. C. H., Wagenaar, N. P., Pluijm, I., Roos-Hesselink, J. W., Essers, J., Danser, A. H. J. Transforming Growth Factor-β and the Renin-Angiotensin System in Syndromic Thoracic Aortic Aneurysms: Implications for Treatment. Cardiovasc Drugs Ther. 2020. doi: 10.1007/s10557-020-07116-4.

70. Touyz, R. M., Schiffrin, E. L. Signal transduction mechanisms mediating the physiological and pathophysiological actions of angiotensin II in vascular smooth muscle cells. Pharmacol Rev. 2000; 52:639–672.

71. Rodríguez-Vita, J., Sánchez-López, E., Esteban, V., Rupérez, M., Egido, J., Ruiz-Ortega, M. Angiotensin II activates the Smad pathway in vascular smooth muscle cells by a transforming growth factor-beta-independent mechanism. Circulation. 2005; 111:2509–2517.

72. Shen, Y. H., LeMaire, S. A., Webb, N. R., Cassis, L. A., Daugherty, A., Lu H. S. Aortic aneurysm and dissections series. Arterioscler Thromb Vas Biol. 2020. 40:e37-e46.

73. Derynck, R., Budi, E. H. Specificity, versatility, and control of TGF-ß family signaling. Sci Signal. 2019; 26:12:eaav5183.

74. Mas-Stachurska, A., Siegert, A. M., Batlle, M., del Blanco, D. G., Meirelles, T., Rubies, C., Bonorino, F., Serra-Peinado, C., Bijnens, B., Baudin, J. et al. Cardiovascular benefits of moderate exercise training in Marfan syndrome: Insights from an animal model. J Am Heart Assoc. 2017; 6:e006438.

75. Gu, X., He, Y., Li, Z., Han, J., & Chen, J. Echocardiographic versus Histologic Findings in Marfan Syndrome. Tex Heart Inst J. 2015; 42:30–34.

76. Gibson, C., Nielsen, C., Alex, R., Cooper, K., Farney, M., Gaufin, D., Cui, J. Z., van Breemen, C., Broderick, T. L., Vallejo-Elias, J. et al. Mild aerobic exercise blocks elastin fiber fragmentation and aortic dilatation in a mouse model of Marfan syndrome associated aortic aneurysm. J Appl Physiol. 2017; 123:147–160.

77. Chen, J., Sawada, H., & Moorleghen, J. Aortic Strain Correlates with Elastin Fragmentation in Fibrillin-1 Hypomorphic Mice. Circ Rep. 2019; 1:199–205.

78. Denby, L., Nicklin, S. A., & Baker, A. H. Adeno-associated virus (AAV)-7 and -8 poorly transduce vascular endothelial cells and are sensitive to proteasomal degradation. Gene Ther. 2005; 12:1534–1538.

79. Maeda, Y., Ikeda, U., Ogasawara, Y., Urabe, M., Takizawa, T., Saito, T., Colosi, P., Kurtzman, G., Shimada, K., & Ozawa, K. Gene transfer into vascular cells using adeno-associated virus (AAV) vectors. Cardiovasc Res. 1997; 35:514–521.

80. Remes, A., Arif, A., Franz, M., Jungmann, A., Zaradki, M., Puehler, T., Heckmann, M. M. B., Frey, N., Karck, M., Kallenbach, K. et al. AAV-mediated AP-1 decoy oligonucleotide expression inhibits aortic elastolysis in a mouse model of Marfan syndrome. Cardiovasc Res. 2021; doi: 10.1093/cvr/cvab012.

81. Davaapil, H., Shetty, D. K., Sinha, S. Aortic “Disease-in-a-Dish”: Mechanistic Insights and Drug Development using iPSC-Based Disease Modeling. Front Cell Dev Biol. 2020; 8:550504. doi: 10.3389/fcell.2020.550504. eCollection 2020.

82. Rurali, E., Perrucci, G. L., Pilato, C. A., Pini, A., Gaetano, R., Nigro, P., Pompilio, G. Precise Therapy for Thoracic Aortic Aneurysm in Marfan Syndrome: A puzzle nearing its solution. Prog Cardiovasc Dis. 2018; 61:328-335.

83. Maguire, E. M., Xiao, Q., Xu, Q. Differentiation and Application of Induced Pluripotent Stem Cell-Derived Vascular Smooth Muscle Cells. Arterioscler Thromb Vasc Biol. 2017; 37:2026-2037.

84. Park, J. W., Yan, L., Stoddard, C., Wang, X., Yue, Z., Crandall, L., Robinson, T., Chang, Y., Denton, K., Li, E. et al. Recapitulating and Correcting Marfan Syndrome in a Cellular Model. Int J Biol Sci. 2017; 13:588-603.

FIGURE LEGENDS

Figure 1. Aortic root dilation progression in MFS mice. Comparative analysis of the aortic root diameter (mm) of wild type (WT) and MFS (*Fbn1*$^{C1041G/+}$) mice of different age groups subjected to transthoracic echocardiography. See Supplementary Table 2 for specific values. Statistical analysis: two-way Anova and Tukey post-test ***$p \leq 0.001$ between WT and MFS, and $^{+++}p \leq 0.001$ between experimental MFS groups.

Figure 2. Aortic root dilation and aortic wall histomorphometry analysis in preventive P144 treatments. Aortic root diameter measured by echocardiography in WT and MFS mice of 4 weeks of age treated with ~~physiological serum (~~PS) or ~~AAVApolinkerP144 (~~P144) for a period of 4 weeks (PE1; **A**) or 20 weeks (PE2; **B**); see respective Supplementary Tables 4 and 5 for specific values. **(C)** Number of large discontinuities in the elastic lamina of the tunica of the ascending aorta (360°) from WT and MFS mice preventively treated (PE1) with PS or P144 expression vector. On the right, representative elastin histological staining (Elastin Verhoeff´s Van Gieson) of the ascending aorta. White arrow indicates a representative large elastic discontinuity counted in the elastic lamina of MFS mouse aortic tissue. Bar 50 µm. **(D)** Tunica media thickness (in µm) of the ascending aorta (360°) from WT and MFS mice preventively treated (PE1) with PS or P144 expression vector. See Supplementary Table 6 for specific values. All results are the mean ± SEM. Two-way Anova and Tukey post-test (A,B,and D) and Kruskal-Wallis and Dunn's post-test (C); *$p \leq 0.05$, ***$p \leq 0.001$ between WT and MFS; $^{+}p \leq 0.05$ and $^{+++}p \leq 0.001$ between experimental MFS groups .

Figure 3. TGFβ signaling in the tunica media after preventive P144 treatment. TGFβ signaling response evaluated by visualization of the nuclear localization of the phosphorylated forms of SMAD2 (pSmad2; **A**) and ERK1/2 (pErk1/2; **B and C**) in the tunica media of ascending aorta. C). Representative immunofluorescence staining for pERK1/2 performed in paraffin-embedded aortae from 4-week-old WT and MFS mice treated with ~~physiological serum (~~PS) or P144 expression vector for 4 weeks (PE1). Results are the mean ± SEM. Kruskal-Wallis and Dunn's post-test; *$p \leq 0.05$ and ***$p \leq 0.001$ between WT and MFS mice; $^{+}p \leq 0.05$ between experimental MFS groups.

Figure 4. Aortic root dilation and aortic wall histomorphometric analysis of palliative P144 treatment (PA) and comparative study with losartan. (A) Aortic root diameter measured by echocardiography in 8 week-old WT and MFS mice treated with ~~physiological serum (~~PS) ~~or AAVApolinkerP144 (~~P144), LOS or P144+LOS for 16 weeks. ~~This is a larger study from the pilot shown in Supplementary Figure 3, where the sample size was increased, LUC expression vector was no longer included, and two new, parallel experimental groups were added: losartan (LOS) and P144 co-treated with LOS (P144+LOS).~~ See Supplementary Table 7 for the specific values of each treatment. **(B)** Tunica media thickness of the ascending aorta (360°) from WT and MFS mice. See Supplementary Table 8 for specific values. **(C)** Number of large discontinuities in the elastic lamina of the tunica of the ascending aorta (360°) from WT and MFS mice. Representative elastin histological staining (Verhoeff´s Van Gieson) of the aortic wall of WT and MFS mice subjected to the treatments indicated are shown

on the right. White arrow indicates an example of a large elastic lamina discontinuity seen in the MFS mouse aortic media. Bar, 50 μm. PS, physiological serum/vehicle; P144, AAVApolinkerP144 expression vector; LOS, losartan; P144+LOS, mice expressing P144 and treated with losartan. Results are the mean ± SEM. Two-way Anova followed by Tukey post-test. **p≤0.01, ***p≤0.001 between WT and MFS mice groups (genotype); $^{+}$p≤0.05, $^{++}$p≤0.01 and $^{+++}$ p≤0.001 between the indicated experimental MFS groups.

Figure 5. TGF-β signaling in the tunica media after palliative treatment with the P144 expression vector. ~~Immunofluorescence~~ analysis of activated phosphorylated forms of SMAD2 **(A)** and ERK1/2 **(B)** localized to nuclei of VSMC of the tunica media of paraffin-embedded aortae from WT and MFS mice subjected to the experimental treatments indicated. Representative immunofluorescence images of each immunostaining and experimental group are shown in Supplementary Figure 4. PS, physiological serum/vehicle; P144, constitutive expression of AAVApolinkerP144 expression vector; LOS, losartan; P144+LOS, constitutively expressing P144 co-treated with losartan. Results expressed as the mean ± SEM. Kruskal-Wallis and Dunn's post-test; *p≤0.05 and ***p≤0.001 between WT and MFS (genotype); ^{+}p≤0.05, $^{++}$p≤0,01 and ^{+++}p≤0.001 between the indicated experimental MFS groups.

Figure 6. *Tgfβ1* and *Tgfβ2* mRNA expression levels in preventive P144 treatments. RT-PCR for *Tgfβ1* and *Tgfβ2* in WT and MFS mice (4 weeks-old) treated with P144 expression vector for 4 weeks (PE1) **(A)** or 20 weeks (PE2) **(B)**. PS, physiological serum/vehicle; P144, constitutive expression of

AAVApolinkerP144 expression vector. Results are the mean ± SEM. ~~Number of mice examined in PE1: WT-PS (n=12), WT-P144 (n=3), MFS-PS (n=12), MFS-P144 (n=4); number of animals evaluated in PE2: WT-PS (n=8), WT-P144 (n=6), MFS-PS (n=9), and MFS-P144 (n=6)~~. mRNA expression values were normalized to *Gapdh* expression as a housekeeping control gene and reported as relative expression compared with WT using the 2-ΔΔCt method. Kuskal-Wallis and Dunn's post-test (A; PE1); and Two-way Anova followed by Tukey post-test (B; PE2). *p≤0.05, **p≤0.01 and ***p≤0.001 between WT and MFS mice groups (genotype); $^{+}$p≤0.05, $^{++}$p≤0.01 and $^{+++}$p≤0.001 between the indicated experimental MFS groups.

FIGURE 1

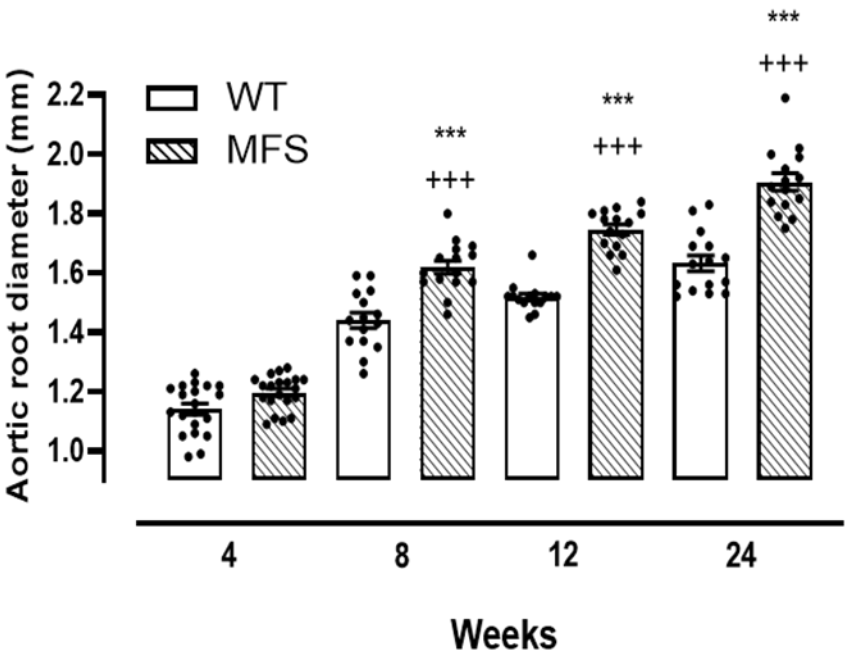
Aortic root diameter (mm)
2.2
2.0
1.8
1.6
1.4
1.2
1.0
WT
MFS
***
+++
***
+++
***
+++
4
8
12
24
Weeks

FIGURE 2

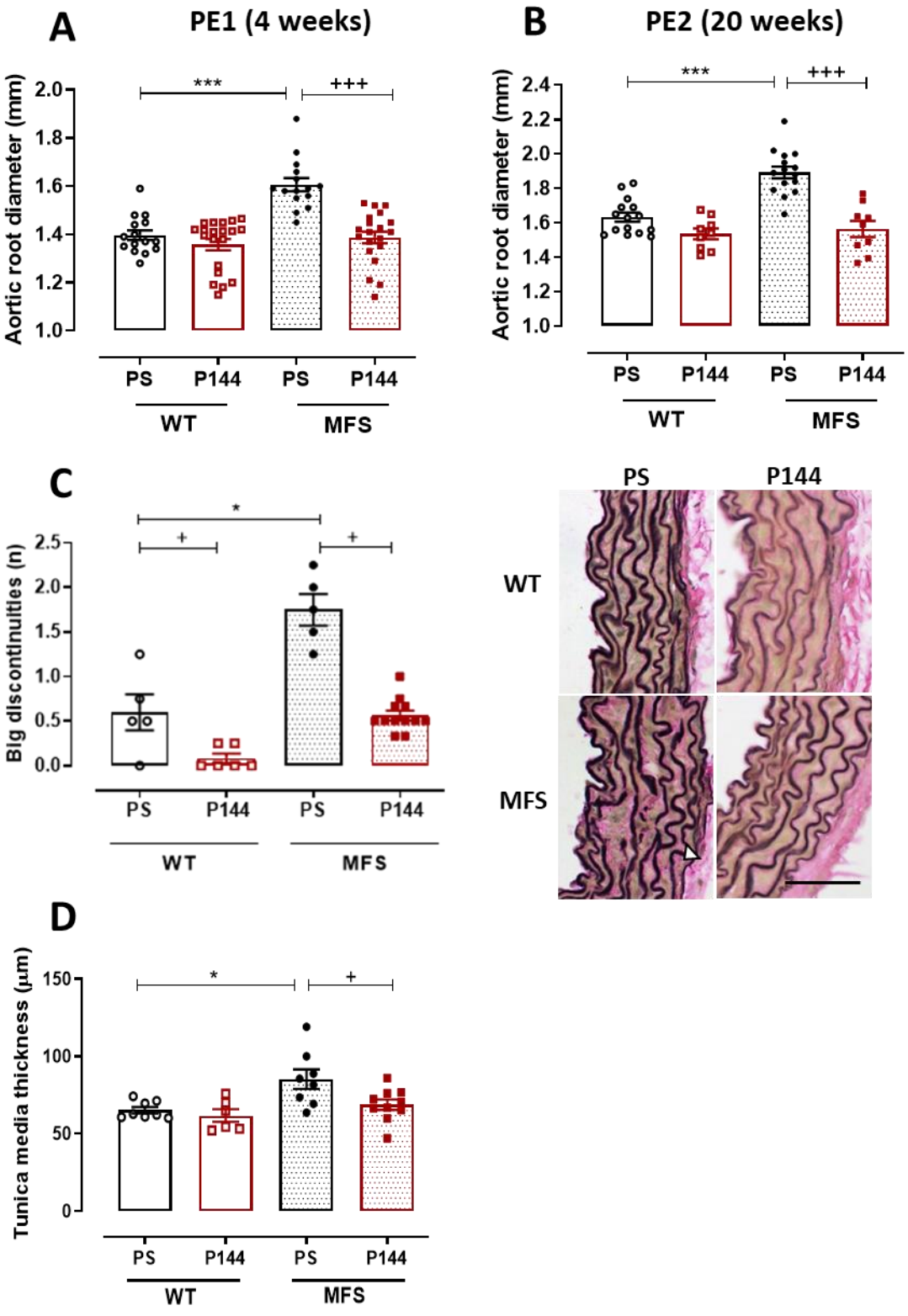
A
PE1 (4 weeks)
Aortic root diameter (mm)
2.0
1.8
1.6
1.4
1.2
1.0
***
+++
PS
P144
PS
P144
WT
MFS
B
PE2 (20 weeks)
Aortic root diameter (mm)
2.4
2.2
2.0
1.8
1.6
1.4
1.2
1.0
***
+++
PS
P144
PS
P144
WT
MFS
C
Big discontinuities (n)
2.5
2.0
1.5
1.0
0.5
0.0
*
+
+
PS
P144
PS
P144
WT
MFS
PS
P144
WT
MFS
D
Tunica media thickness (µm)
150
100
50
0
*
+
PS
P144
PS
P144
WT
MFS

FIGURE 3

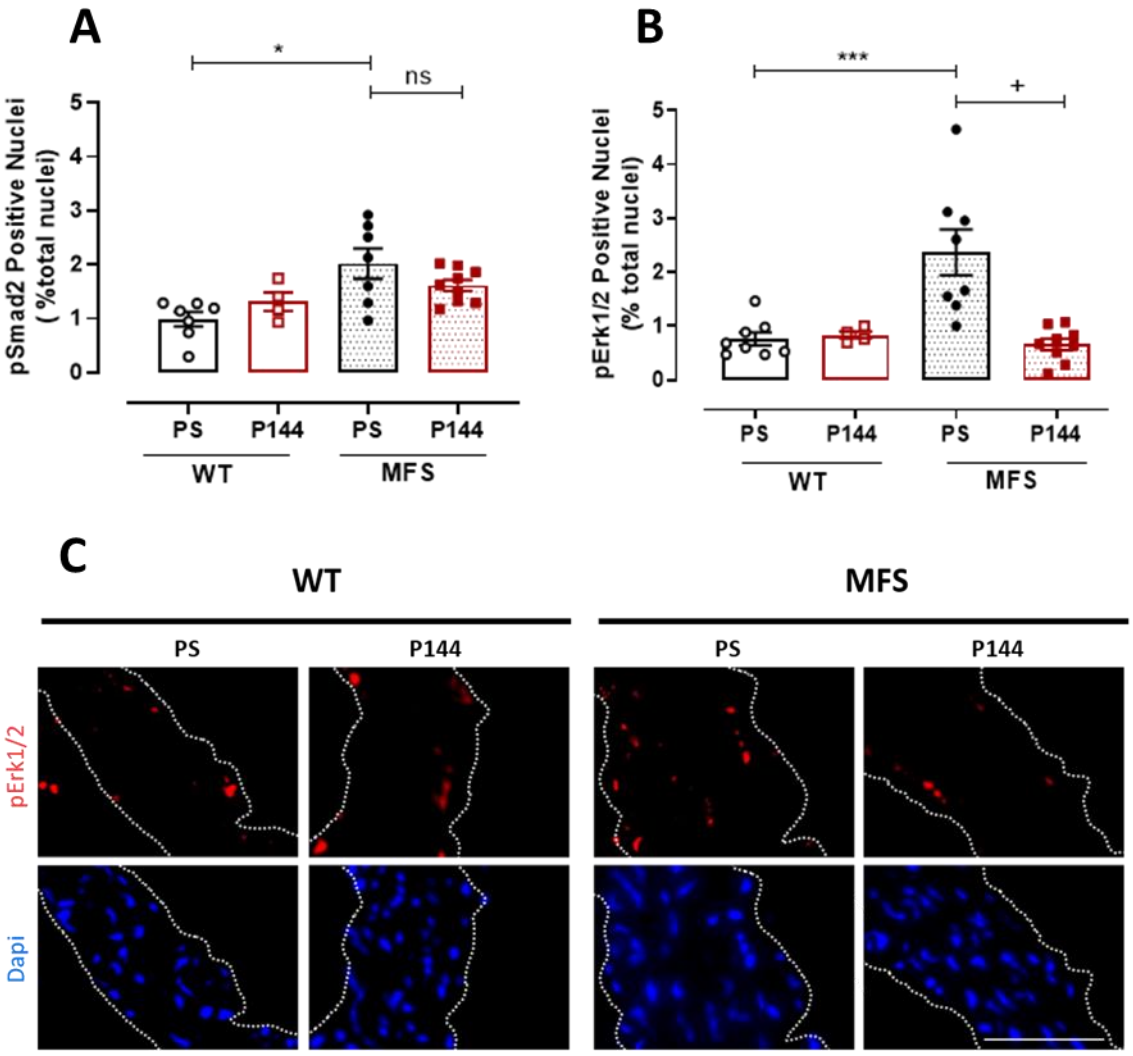
A
*
ns
pSmad2 Positive Nuclei
(%total nuclei)
0
1
2
3
4
5
PS
P144
PS
P144
WT
MFS
B
***
+
pErk1/2 Positive Nuclei
(% total nuclei)
0
1
2
3
4
5
PS
P144
PS
P144
WT
MFS
C
WT
MFS
PS
P144
PS
P144
pErk1/2
Dapi

FIGURE 4

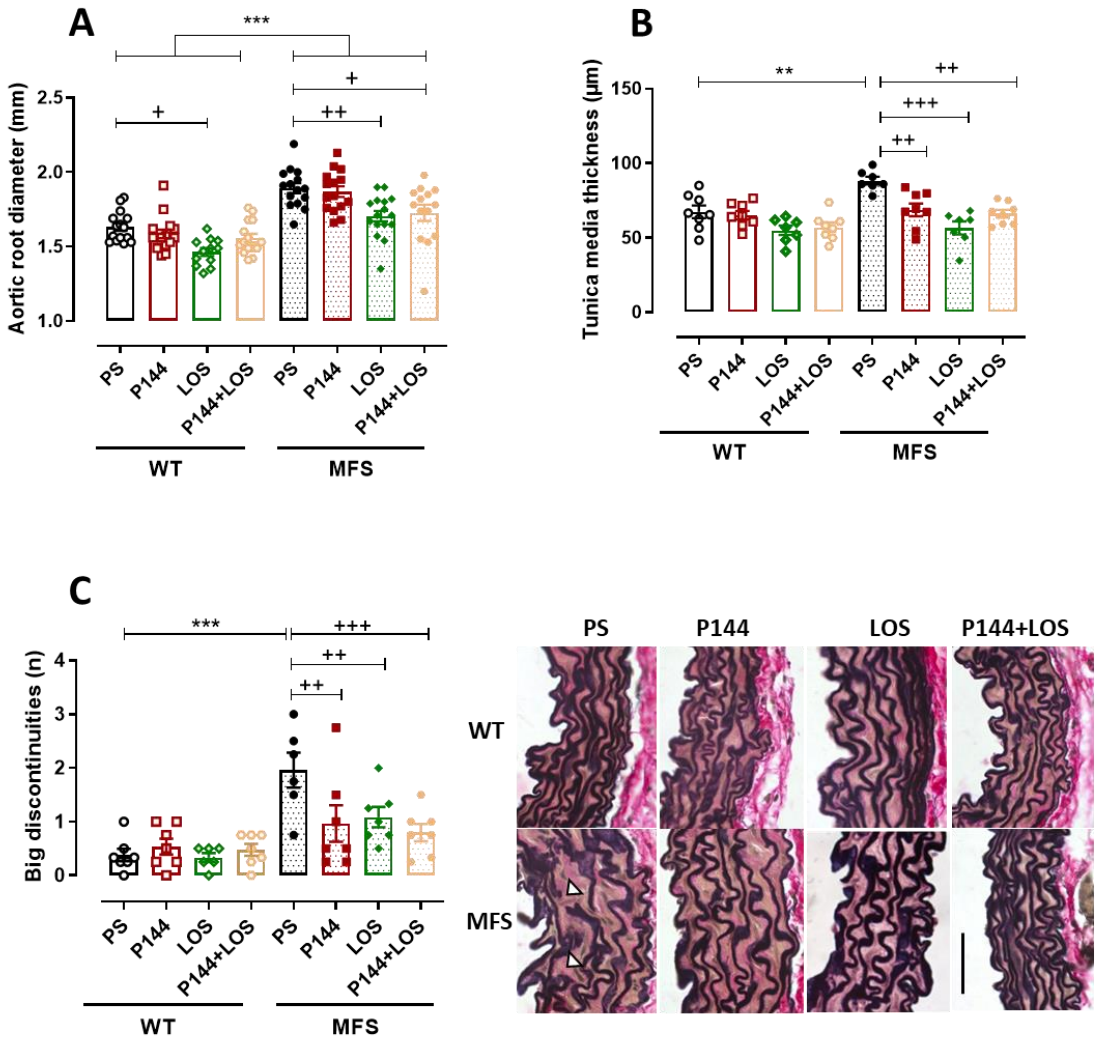
A
Aortic root diameter (mm)
2.5
2.0
1.5
1.0
***
+
+
++
PS
P144
LOS
P144+LOS
PS
P144
LOS
P144+LOS
WT
MFS
B
Tunica media thickness (µm)
150
100
50
0
**
++
+++
++
PS
P144
LOS
P144+LOS
PS
P144
LOS
P144+LOS
WT
MFS
C
Big discontinuities (n)
4
3
2
1
0
***
+++
++
++
PS
P144
LOS
P144+LOS
PS
P144
LOS
P144+LOS
WT
MFS
PS
P144
LOS
P144+LOS
WT
MFS

FIGURE 5

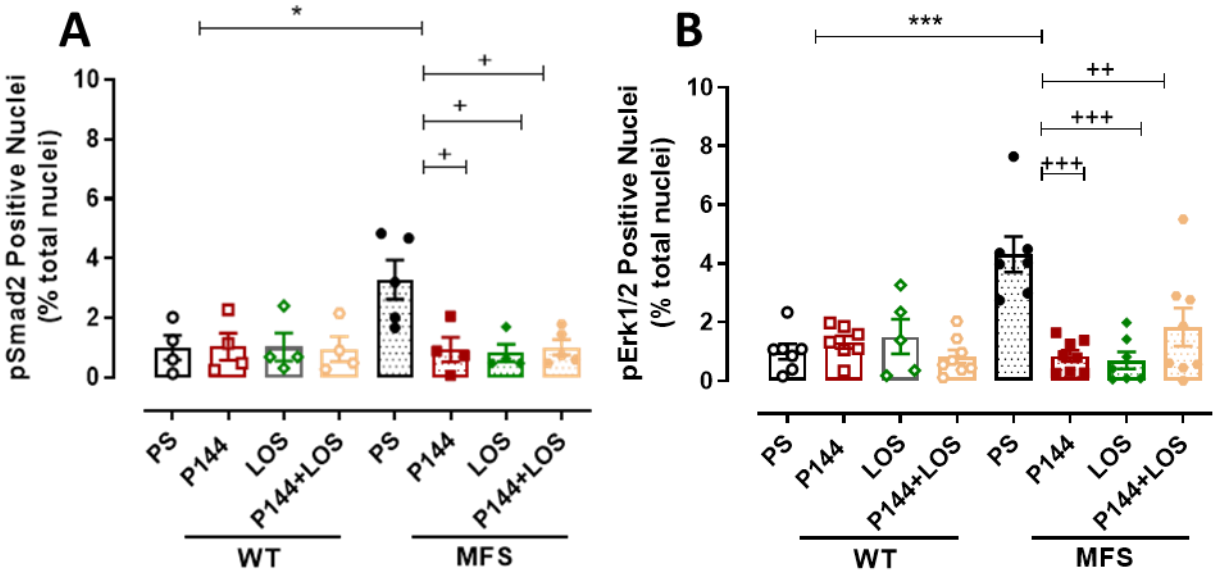
A
pSmad2 Positive Nuclei
(% total nuclei)
10
8
6
4
2
0
*
+
+
+
PS
P144
LOS
P144+LOS
PS
P144
LOS
P144+LOS
WT
MFS
B
pErk1/2 Positive Nuclei
(% total nuclei)
10
8
6
4
2
0
***
++
+++
+++
PS
P144
LOS
P144+LOS
PS
P144
LOS
P144+LOS
WT
MFS

FIGURE 6

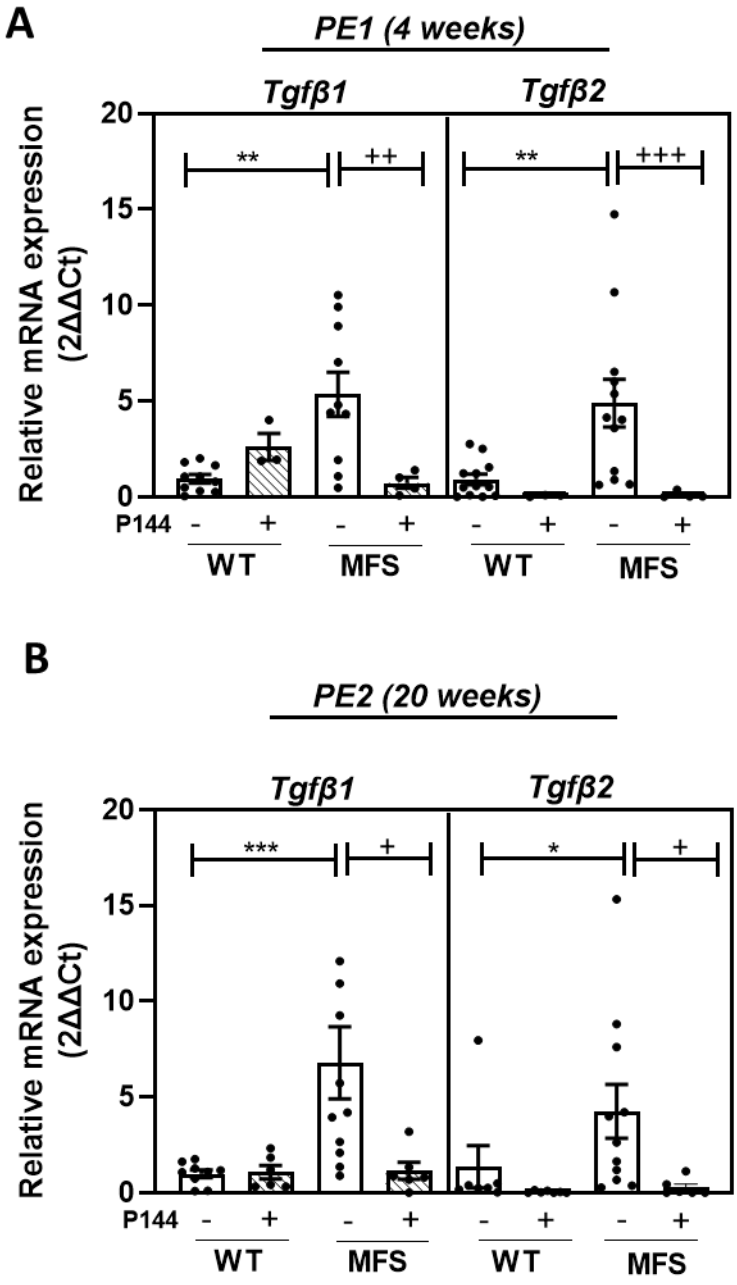
A
PE1 (4 weeks)
Tgfβ1
Tgfβ2
Relative mRNA expression (2ΔΔCt)
20
15
10
5
0
**
++
**
+++
P144 - + - + - + - +
WT
MFS
WT
MFS
B
PE2 (20 weeks)
Tgfβ1
Tgfβ2
Relative mRNA expression (2ΔΔCt)
20
15
10
5
0
***
+
*
+
P144 - + - + - + - +
WT
MFS
WT
MFS